NIH-PA Author Manuscript

Sustained expression of interleukin-1β in mouse hippocampus impairs spatial memory

Amy H. Moore[1,*], **Michael Wu**[2], **Solomon S. Shaftel**[2], **Kaylan A. Graham**[1], and **M. Kerry O'Banion**[2,3]

[1] Department of Biology, Santa Clara University, Santa Clara, CA 95053

[2] Department of Neurobiology & Anatomy, University of Rochester School of Medicine and Dentistry, Rochester, NY 14642

[3] Department of Neurology, University of Rochester School of Medicine and Dentistry, Rochester, NY 14642

Abstract

Glial activation and neuroinflammation occur in neurodegenerative disease and brain injury, however their presence in normal brain aging suggests that chronic neuroinflammation may be a factor in age-related dementia. Few studies have investigated the impact of sustained elevation of hippocampal interleukin-1β, a pro-inflammatory cytokine upregulated during aging and Alzheimer's disease, on cognition in mice. We utilized the IL-1β[XAT] transgenic mouse to initiate bilateral hippocampal overexpression of interleukin-1β to determine the influence of sustained neuroinflammation independent of disease pathology. Fourteen days following transgene induction, adult male and female IL-1β[XAT] mice were tested on non-spatial and spatial versions of the Morris water maze. For the spatial component, one retention trial was conducted forty-eight hours after completion of a 3-day acquisition protocol (8 trials per day). Induction of IL-1β did not impact non-spatial learning, but was associated with delayed acquisition and decreased retention of the spatial task. These behavioral impairments were accompanied by robust reactive gliosis and elevated mRNA expression of inflammatory genes in the hippocampus. Our results suggest that prolonged neuroinflammation response *per se* may impact mnemonic processes and support the future application of IL-1β[XAT] transgenic mice to investigate chronic neuroinflammation in age- and pathology-related cognitive dysfunction.

Keywords

neuroinflammation; water maze; IL-1β[XAT] transgenic mouse; hippocampus

---

Chronic neuroinflammation is a prominent feature of Alzheimer's disease (AD) and is believed to contribute to the molecular cascade that ultimately manifests as cognitive dysfunction. It is well known that the single most important risk factor for AD is age. One reason for this association is that the progression from initial pathophysiological event to clinical detection is

---

*Corresponding author: Amy H. Moore, Ph.D., Department of Biology, Carleton College, One North College Street, Northfield, MN 55057, Phone: 1.507.222.5981, Fax: 1.507.222.5757, amoore@carleton.edu.
Neuroscience Section Editor: Behavioral Neuroscience

likely to be on the order of decades. Although glial activation is influenced by neuronal plaques and tangles, its presence in the aged brain (Nichols et al., 1993; Perry et al., 1993; Conde and Streit, 2006; Beach et al., 2007; Gavilan et al., 2007), independent of AD-like neuropathology, suggests that chronic neuroinflammation may be an initial component of and factor in age-related dementia (Cagnin et al., 2001; Weaver et al., 2002).

Reactive glia produce a variety of molecules that trigger and contribute to chronic neuroinflammation. Termed "the cytokine cycle" (Griffin et al., 1998), pro-inflammatory cytokines participate in a spectrum of signaling events that continuously feedback and influence each other. Microglial-derived IL-1β appears to be a driving force in this process. IL-1β has been previously shown to be a potent immunomodulating cytokine that induces multiple inflammatory mediators in astrocytes and neurons (Mrak et al., 1995). IL-1β overexpression is a consistent feature of post-mortem AD brain, with double-labeling immunohistochemical studies localizing IL-1 to plaque-associated microglia (Griffin et al., 1995; Griffin et al., 2000; Shaftel et al., 2008). In addition to initiating and sustaining inflammation-related events and modulating neurons, IL-1β appears to have direct relation to pathophysiological alterations in AD (for review, refer to (Moore and O'Banion, 2002; Shaftel et al., 2008)). Its regional expression around plaques and its temporal profile of immunoreactivity relative to pathology implicates IL-1β as a mediator of plaque and tangle formation. Not restricted to AD pathology, increased IL-1β is found in the hippocampus of aged rats (Murray and Lynch, 1998; Griffin et al., 2006), reinforcing the hypothesis that chronic neuroinflammation may be initiated by the normal process of aging. However, the role of chronic neuroinflammation in cognitive dysfunction has yet to be clearly determined.

Understanding the role of neural expression of pro-inflammatory molecules in memory processes has been addressed in animal models. Numerous investigators have described learning and memory impairments associated with acute central IL-1β induction (≤5 days) following peripheral lipopolysaccharide (LPS) stimulus (Shaw et al., 2001; Yirmiya et al., 2002; Sparkman et al., 2005b; Sparkman et al., 2005a; Wu et al., 2007) and direct central administration of IL-1β (Yirmiya et al., 2002; Goshen et al., 2007; Hein et al., 2007). Impaired hippocampal-dependent performance has also been reported at 24 hours following intracerebroventricular infusion of IL-1 receptor antagonist (IL-1ra; Yirmiya et al., 2002) and in transgenic mice lacking expression of IL-1ra (Avital et al., 2003), further suggesting a role of constitutive IL-1 signaling in cognition. However, only a limited number of studies address the adult onset and ongoing presence of neuroinflammation that is representative of aging and AD. Substantial research has been conducted in a rat model of chronic (> 7 days) neuroinflammation (Hauss-Wegrzyniak et al., 1998a; Hauss-Wegrzyniak et al., 1998b; Hauss-Wegrzyniak et al., 2000a; Hauss-Wegrzyniak et al., 2000b) and transgenic mouse models of AD neuropathology. Yet, considering the prevalence of mice as the standard research model given the potential and ease of genetic manipulation, data are sparse on the effect of prolonged region-specific glial activation and elevated IL-1β brain concentrations *per se* on behavior in adult mice. Therefore, we utilized a recently established transgenic mouse model (IL-1β^{XAT}; Shaftel et al., 2007b; Shaftel et al., 2007a) to determine the effect of induced human IL-1β in the hippocampus on spatial memory in adult C57BL/6 mice. Our results suggest that sustained (14 days) elevation of hippocampal hIL-1β and the accompanying increase in pro-inflammatory molecules drive mnemonic deficits, establishing the IL-1β^{XAT} mouse as a valid model to investigate the consequence of chronic hIL-1β expression.

EXPERIMENTAL PROCEDURES

Subjects

IL-1β^{XAT} Transgenic mice—Twenty-two IL-1β^{XAT} mice (13 male and 9 female) were used in this study. Creation and genotyping of the IL-1β^{XAT} mice on a C57BL/6 background have

been described previously (Shaftel et al., 2007b; Shaftel et al., 2007a). Briefly, the IL-1β[XAT] mice harbor a transgene construct consisting of a murine GFAP promoter (Stalder et al., 1998), loxP flanked transcriptional stop, and downstream ssIL-1β transgene coding for the signal sequence from the human IL-1ra (75 bp) fused to the cDNA sequence of human mature IL-1β (464 bp) (Wingren et al., 1996). Transgene activation occurs upon feline immunodeficiency virus (FIV)-Cre recombinase protein (Cre) mediated excision of a transcriptional stop. All animal procedures were reviewed and approved by the Institutional Animal Care and Use Committee at University of Rochester and Santa Clara University for compliance with federal regulations before the initiation of the study.

Feline immunodeficiency virus—The construction and packaging of FIV-Cre has been described previously (Lai et al., 2006b). Briefly, the FIV-Cre virus encodes the nuclear localization sequence (nls), Cre, and V5 epitope tag under the control of a cytomegalovirus promoter. FIV-Cre and FIV-green fluorescent protein (GFP; System Biosciences, Mountain View, CA) were packaged to a final titer of 1×10^7 infectious viral particles (IVP) per ml. *In vivo* stereotactic injections were performed at 12 weeks of age and used 1.5 μl of virus to deliver 1.5×10^4 IVP to the mouse hippocampus. Viral titers were established in the 293[FT] cell line using an anti-V5 antibody (Invitrogen, Carlsbad, CA) or GFP fluorescence.

Stereotactic injections—Intrahippocampal injections were performed as described previously (Shaftel et al., 2007b; Shaftel et al., 2007a). Briefly, mice were anesthetized with 1.75% isoflurane in 30/70% oxygen/nitrogen gas. While secured to a Kopf stereotaxic apparatus in a biosafety level 2 approved facility, two 0.5 mm burr holes were drilled in the skull at −1.8 mm caudal and 1.8 mm horizontal on each side of bregma. A pre-loaded 33 gauge needle was lowered first into the right hippocampus, 1.75 mm from the brain surface over 2 min after which 1.5 μl of virus was injected at a constant rate over 10 min. After allowing 5 min for diffusion of the virus, the needle was raised over 2 min. A second injection was performed in an identical manner on the contralateral side. The burr holes were sealed with bone wax and the scalp incision was closed with 6-0 nylon suture (Ethicon, Somerville, NJ). Control animals received bilateral intrahippocampal injections of FIV-GFP using the same procedures.

Behavioral apparatus & procedures

Fourteen days after bilateral hippocampal injections, mice were tested on non-spatial and spatial learning using the Morris water maze (MWM) adapted for mice (Vorhees and Williams, 2006). The MWM consisted of a black, plastic circular tub (88 cm diameter, 12 cm deep) filled with water (25±1°C) made opaque using non-toxic white tempera paint. A removable 10 cm^2 plexiglass platform with weighted base was placed in the water approximately one centimeter below the surface of the water. Visual cues were placed in various locations of the testing room. A ceiling mounted digital camera and ANY-Maze® software (Stoelting Co., Chicago, IL) was used to automatically collect data during behavioral testing. Both non-spatial (visible platform) and spatial (hidden platform) versions of the test were conducted for each mouse.

Shaping—One day prior to training, mice were introduced (shaped) to the water maze by placing the animal on the visible escape platform for 10 seconds (s) and then placing the animal in the water at successively greater distances from the platform over three 45 s trials. The mouse was guided to the escape platform if the trial ended without the mouse finding the platform. General motor ability was observed and swim speed was measured.

Non-spatial Task—One day following shaping, animals were trained to escape to a visible platform in the water maze during two sets of four trials with inter-trial and inter-set intervals

of 5 and 120 min, respectively. In this non-spatial task, the platform was made visible by raising it 1 cm above the surface of the water and marking it with patterned tape and a perpendicular cue. For each trial, the mouse was placed in the maze (facing tub wall) at the same drop point with the position of the visible platform alternating between quadrants.

Spatial Task—One day following acquisition of the non-spatial task, each mouse experienced three days of spatial training in locating a hidden escape platform. Each training day consisted of two sets of four trials with inter-trial and inter-set intervals of 5 min and 120 min, respectively. The starting point of each trial varied between four designated drop points. After completion of the three-day training protocol, one final trial was performed forty-eight hours later to test spatial memory retention.

For all trials (non-spatial and spatial), a maximum of 45 s was allowed for the mouse to find the hidden platform. The trial automatically ended when the mouse remained on the hidden platform for 3 s. If the trial ended without the mouse finding the escape platform, the investigator guided the mouse to the platform where it remained for 10 s. For all testing phases, mice were placed in a heated holding chamber for inter-trial intervals and, upon demonstrating normal behavior (e.g. grooming, rearing, exploring), their home cages for inter-set intervals.

Latency (duration of trial), path length (distance traveled), swim speed, proportion of time and distance spent in the periphery and average distance from the platform were recorded per trial.

Tissue collection

Within twenty-four hours of spatial memory retention trials, mice were anesthetized with ketamine (i.p. 60–90 mg/kg) plus xylazine (i.p. 4–8 mg/kg) and sacrificed by intracardiac perfusion with chilled 0.15 M sodium phosphate buffer (pH 7.2) containing 0.1% sodium nitrite. The perfusion pressure was monitored to insure that it did not exceed 90 mm/Hg. The brain was removed and hemisected. For immunohistochemical studies, one hemisphere was post-fixed in chilled 4% paraformaldehyde for 24 hours. For all remaining analyses, the hippocampus was dissected from the remaining hemisphere, immediately snap-frozen in chilled isopentane, and stored at −80° C until processing.

Immunohistochemistry

Following 24 h immersion fixation and equilibration with 30% sucrose in 0.15 M phosphate buffer, brains were frozen and sectioned at 30 μm on a sliding microtome (Microm HM430). The sections were stored in cryoprotectant solution until ready for immuno-histochemical (IHC) processing. Antibody binding of major histocompatibility complex class II (MHC-II) (1:6000, #553549 BD Biosciences, San Jose, CA) and ionized calcium binding adaptor molecule-1 (Iba-1) (1:5000 #019-19741 Wako) for microglia/macrophages, glial fibrillary acidic protein (GFAP) (1:6000 #Z0334 Dako) for astrocytes, and 7/4 (1:5000, #MCA771B Serotec) for neutrophils was visualized using Elite avidin –biotin and 3,3-diaminobenzidine (Vector Laboratories, Burlingame, CA). Terminal deoxynucleotidyl transferase mediated dUTP nick end labeling (TUNEL) (ApopTag; Chemicon) was performed according to the manufacturer's protocol along with antibody binding of NeuN (1:2000 #MAB377B Chemicon) and visualization with a streptavidin 647 Alexa Fluor antibody (1:400 #S32357 Invitrogen).

Light microscopic images were acquired at 200x magnification on an Axioimager (Zeiss, Thornwood, NY) microscope equipped with a Retiga-2000R camera and QCapture PRO software (Qimaging, Surrey, BC, Canada). To determine degree of immunoreactivity of MHC-II, Iba-1, and GFAP, images of the dorsal hippocampus were captured using fixed exposure times across all sections within each protein of interest. All light microscopy images were converted to a global gray scale (0–255 levels). A threshold was applied to all images to discern

immunoreactive cells from background. Total percent immunoreactive area was determined for the molecular layer of the dentate gyrus, and the stratum radiatum of CA1 and CA3 for each animal by averaging three fixed-area regions of interest for each hippocampal region (Image J, NIH, Bethesda, MD).

Fluorescent images were captured using an AttoArc 2 (Zeiss) mercury lamp, Sensicam QE camera (Cooke, Romulus, MI), and Slidebook 5.0 software (Intelligent Imaging, Denver, CO) in Macintosh OS 10.4. Equivalent exposure times were used when comparing animal groups. For TUNEL/NeuN counting, captures of a representative section containing the dentate gyrus from each animal were taken at 20x magnification and analyzed to quantify TUNEL positive cells. For illustrative purposes, confocal images were taken on an Olympus FV1000 laser scanning confocal microscope at 20x and 240x magnification and NeuN was pseudo-colored cyan for better visualization. Final images were generated in Photoshop CS2 and layout performed in Illustrator CS2 (Adobe, San Jose, CA).

Real-time RT-PCR

General quantitative real-time RT-PCR (qRT-PCR) procedures have been described in detail previously (Shaftel et al., 2007b; Shaftel et al., 2007a). Briefly, RNA from one hippocampus per animal was isolated using Trizol (Invitrogen). cDNA was generated using oligo-dT and random hexamer primers, and Superscript III (Invitrogen). Quantification of relative mRNA abundance per animal was determined using custom designed primers (Invitrogen) and FAM 490 probes (Biosearch Technologies, Novato, CA) with the iCycler (Bio-Rad, Hercules, CA). Reactions were performed in a final volume of 20 μl using iQ Supermix (Bio-Rad) and 5 nM FITC dye as follows: 95°C for 3 min, followed by 50 cycles of 95°C for 15 s, and 60°C for 1 min. Ribosomal 18s housekeeping gene was used to normalize determinations of mRNA abundance. Sequences of primers used for GFAP, mouse IL-1α, mouse IL-1β macrophage-inflammatory protein (MIP)-2, MHC-II, monocyte chemoattractant protein 1 (MCP-1), KC (CXCL1), CCR2, CXCR2, and 18s rRNA are presented in Table 1.

Statistical Analysis

Non-spatial and spatial water maze measurements were averaged within each itreatment group (FIV-GFP or FIV-Cre) for each trial (non-spatial) or acquisition day (spatial). Two-way analyses of variance (ANOVA) were performed with treatment group and sex as the independent variables, and trial (non-spatial) or day (spatial) as the repeated measure (SPSS, Inc; Chicago, IL). For all molecular comparisons, two-tailed student t-tests were used to evaluate changes in immunoreactivity and mRNA levels between control (FIV-GFP) and experimental (FIV-Cre) groups, with each animal represented by one measurement within the comparison. Correlation and regression analyses were done to assess the relationship between memory performance and molecular markers of neuroinflammation.

Data are presented as mean across all animals within a treatment group ± standard error of the mean (SEM). An alpha level of 0.05 was necessary to reject the null hypothesis and to consider the data statistically significant.

RESULTS

Memory performance in water maze

To model sustained overexpression of IL-1β within the CNS, we took advantage of the recently described IL-1β^{XAT} transgenic mouse (Shaftel et al., 2007a). IL-1β^{XAT} mice harbor a transgene cassette featuring a GFAP promoter, loxP flanked transcriptional stop, and downstream transcriptionally silent human IL-1β transgene (hIL-1β). Previous characterization of this model showed that stereotactic injection of an FIV virus expressing Cre recombinase (FIV-

Cre) into the mouse brain elicits transgene induction lasting months after viral transduction that is associated with prominent, long-lasting glial reactivity. To investigate whether hIL-1β overexpression in the hippocampus influenced mnemonic behavior during peak transgene expression, IL-β^{XAT} transgenic mice that received bilateral intrahippocampal injections of FIV-Cre or FIV-GFP were assessed on non-spatial and spatial memory using the Morris water maze. All animals completed shaping without swimming difficulty. No sex difference on latency or path length measurement was detected in either behavioral task within the FIV-GFP mice ($p>0.05$). Furthermore two-way ANOVA (treatment group and sex as fixed factors) revealed no effect of sex on behavioral indices. Therefore, the animals were pooled and sex was not considered a between-subject factor.

Non-spatial Memory—To confirm that motivation, visual ability, and motor skills were intact (Vorhees and Williams, 2006), we assessed the animals on a cued non-spatial visual task that is not dependent on hippocampal function. A significant effect of trial was observed on latency ($F_{7,14} = 6.12$, $p<0.01$) and path length ($F_{7,14} = 4.27$, $p<0.01$) (Figure 1), indicating acquisition of the task. No significant difference in acquisition rates of either index was observed between the two treatment groups ($F_{1,20} < 0.99$, $p=$ NS).

Spatial Task—To determine if intrahippocampal FIV-Cre-injections influenced hippocampal-dependent memory, mice were trained to find a hidden platform in opaque water based on spatial cues. ANOVA with repeated measures revealed significant effects of day on latency ($F_{2,19}=19.7$, $p<0.001$), and path length ($F_{2,19}=36.5$, $p<0.001$), representing acquisition of the task (Figure 2). Path length, an index independent of swim speed, was used in further analyses since a significant effect of day ($F_{2,19}=7.4$, $p<0.01$) and a notable interaction between day × treatment ($F_{2,19}=3.29$, $p=0.059$) on swim speed were observed.

Although no main effect of treatment on path length measures was seen over all training days, ANOVA with repeated measures indicated a significant day × treatment interaction on path lengths ($F_{2,19}=4.05$, $p≤0.05$). Post-hoc analysis revealed that FIV-Cre-injected IL-1β^{XAT} mice tended to swim greater distances (4.64 ± 0.40 m) on the first day of spatial training when compared to path lengths from those mice receiving FIV-GFP (3.61 ± 0.39 m; $t_{20}= -1.83$, $p=0.083$). For descriptive purposes, we compared the effect of treatment within each block of 4 trials (set) and found that FIV-Cre mice recorded greater path lengths on the first sets of Day 1 ($t_{20}=-1.973$, $p=0.062$) and Day 2 ($t_{20}=-0.994$, $p=0.072$) that approached significance (Figure 2B), suggesting impairment in spatial acquisition and overnight retention, respectively.

In addition to latency and path length, we further characterized spatial learning ability by calculating the mean distance from platform center for each acquisition trial (Vorhees and Williams, 2006). Distance from the platform significantly decreased across days ($F_{2,19}= 8.015$, $p<0.01$). However, an interaction between day X treatment was noted ($F_{2,19}= 2.94$, $p=0.077$), largely due to FIV-Cre mice searching farther from the hidden platform on Day 2 ($t_{20}=-2.661$, $p<0.05$) relative to FIV-GFP mice (Figure 3). Upon completion of the final set of acquisition trials (Day 3), all mice performed at similar levels.

Spatial memory retrieval was determined by administering one retention trial 48 hours following the 3-day acquisition protocol. Although there was no difference in performance on the last set of acquisition trials, FIV-Cre-injected IL-1β^{XAT} mice exhibited impaired memory retention of the spatial task with increased path lengths on the retention trial (3.78 ± 1.05 m) relative to FIV-GFP-injected mice (1.65 ± 0.32 m; $t_{20}=2.09$, $p<0.05$) (Figure 4). Given the previous analyses on spatial learning, we compared the path lengths recorded during the retention trial with those from sets of acquisition trials that tended toward significance. The path lengths of the initial set of Day 2 acquisition trials (representative of overnight retention) were significantly correlated with 48 hour retention trial distances ($r_{22}=0.49$, $p<0.05$)

Molecular confirmation of neuroinflammation

To determine if behavioral differences were correlated with molecular markers of neuroinflammation, brains were collected within 24 hours following completion of the 48-hour retention trial. One hemisphere from each mouse was fixed, frozen and sectioned for immunohistochemical detection. The hippocampus from the remaining hemisphere was analyzed for mRNA expression using qRT-PCR.

A hallmark of chronic neuroinflammation is reactive gliosis, as characterized by changes in glial cell surface marker expression and morphology. Evaluation of microglial activation in all animals using immunoreactivity to major histocompatibility complex class II (MHC-II), a protein upregulated on activated macrophages/microglia, revealed a distinct difference between experimental groups. The FIV-GFP-injected animals exhibited minimal staining across all brain regions examined (Figure 5A). Clear positive staining was detected in all regions of the FIV-Cre-injected IL-1β^{XAT} hippocampus, indicating morphological changes and focal neuroinflammation (Figure 5B). Densitometric analysis supported visual observation of elevated immunoreactivity OF MHC-II associated with hIL-1β transgene induction, with significantly increased percent area reaching threshold optical density (tOD) in FIV-Cre hippocampal regions(molecular layer 32.0%±8.0 vs. 1.0%±0.3; CA1 stratum radiatum 46.8% ±12.0 vs. 10.3%±9.5; CA3 stratum radiatum 30.3%±8.0 vs. 0.7%±0.4;Figure 5C). Furthermore, qRT-PCR analysis showed a significant increase in MHC-II mRNA expression in FIV-Cre-injected IL-1β^{XAT} hippocampus (91.8 ± 25.0 relative to 1±0.31 for control, $t_{20}=$ −3.994, $p<0.05$; Figure 5D).

To complement MHC-II immunoreactivity, additional sections from a subset of animals (n=4 per experimental group) were immunohistochemically stained with an antibody to Iba-1 and GFAP and displayed microglia and astrocytic hypertrophy, respectively, when comparing FIV-Cre (Figure 6B,E) to FIV-GFP hippocampus (Figure 6A,D). Analysis of tOD confirmed a significant increase in Iba-1 immunoreactivity (molecular layer 64.9%±0.8 vs. 27.5%±4.1; CA1 stratum radiatum 44.0%±5.2 vs. 24.6%±2.6; CA3 stratum radiatum 61.1%±10.6 vs. 18.6%±3.9; Figure 6C). GFAP immunoreactivity did not significantly differ between experimental groups using this subset of animals (molecular layer 29.8%±5.1 vs. 20.4%±4.2; CA1 stratum radiatum 31.0%±7.7 vs. 20.8%±3.2; CA3 stratum radiatum 40.9%±12. vs. 18.6% ±3.9; Figure 6F), however GFAP mRNA expression was significantly elevated in FIV-Cre injected mice (1.7 ± 0.2 relative to 1 for control, $t_{20}=$ −2.38, $p<0.05$; Figure 6G).

In addition, tissue sections stained with antibody 7/4 demonstrated substantial neutrophil infiltration in FIV-Cre-injected IL-1β^{XAT} mice (Figure 7) that was associated with relative increases in hippocampal mRNA expression of neutrophil recruitment-associated chemokine receptors CCR2 (3.0 ± 0.5, $t_{20}=$ −4.49, $p<0.05$) and CXCR2 (24.0 ± 4.6, $t_{20}=$−5.46, $p<0.05$).

Additional measurement of inflammation-related gene expression in hippocampal tissue demonstrated mRNA levels (relative to 1 for all controls) of mIL-1α (3.1 ± 0.8), mIL-1β (22.9 ± 6.0), MIP-2 (3.2 ± 0.8), MCP-1 (147.0 ± 34.8) and KC (16.8 ± 2.9), were significantly increased in FIV-Cre-injected mice relative to FIV-GFP-injected controls (−6.0 < t_{20} < -2.4, $p<0.05$; Figure 8). These data demonstrate endogenous interleukin (IL-1s) and chemokine (MIP, MCP, and KC) induction that is common to inflammatory conditions.

Relationship between memory retention and mRNA expression

To assess the relationship between inflammatory mRNA expression and mouse memory performance, we performed a Pearson product moment correlation between each gene expression profile and the 48 hour-retention trial path length within animals. As expected, significant correlations were observed between memory performance and MCP-1 ($r_{21}=0.656$,

p<0.001), MIP-2 (r_{20}=0.576, p<0.01), mIL-1α (r_{20}=0.695, p<0.001), mIL-1β (r_{20}=0.529, p<0.05), and CCR2 (r_{22}=0.543, p<0.001). However, when restricting the analysis to FIV-Cre injected animals, only mIL-1α expression was significantly correlated with retention path length (r_{10}=0.659, p<0.05). Furthermore, forward stepwise multiple regression analysis across all animals with mRNA expression profiles included as predictor variables indicated that mIL-1α significantly predicted retention swim distance (β = 0.749, t_{17}=4.516, p<0.001).

Evaluation of neuronal cell death

Double-label fluorescent immunohistochemistry was performed to assess the impact of hIL-1β induction on neuronal loss. A significant increase in cells positive for the apoptotic marker TUNEL was observed in the hippocampus of FIV-Cre mice (28.9±5.7 per 10^5 μm^2; Figure 9B) relative to FIV-GFP-injected controls (1.0±0.3; p<0.001; Figure 9A). Because TUNEL immunoreactivity was rarely co-localized with neuronal marker NeuN, all TUNEL-positive cells in the dentate gyrus granular layer were quantified. TUNEL+ cells in the dentate gyrus granular layer represented only 4% of all TUNEL+ cells in the FIV-Cre mice (Figure 9C), a proportion that was not statistically significant to those detected in FIV-GFP mice (p>0.05).

DISCUSSION

Chronic neuroinflammation is a common component of several neurodegenerative diseases that are associated with cognitive deficits, including Alzheimer's disease, as well as aging. In order to determine the influence of sustained expression of pro-inflammatory molecule IL-1β on spatial memory in the absence of disease pathology, we utilized the recently characterized IL-1β^{XAT} mouse (Shaftel et al., 2007a). This transgenic mouse model allows for controlled initiation of IL-1β transcription leading to localized neuroinflammation. We observed that induction of hIL-1β in the hippocampus for 14 days by a single FIV-Cre injection influenced acquisition of the spatial learning task as reflected by increased path lengths and distance away from the escape platform during the initial trials on the first two days of training. The delay in spatial learning was associated with significant increase in path lengths observed on the 48-hour memory retention trial. These data suggest that sustained production of IL-1β hinders acquisition and long-term memory retention on a spatial task, similar to the impairment of contextual memory consolidation seen in rats receiving acute central administration of IL-1β (Barrientos et al., 2002).

The effect of chronic neuroinflammation on cognition has been previously addressed using extended infusion of pro-inflammatory molecules into the rodent brain. Hauss-Wegrzyniak and colleagues described spatial memory deficits following prolonged administration of LPS into the fourth ventricle of rat that were associated with glial activation and degeneration of hippocampal pyramidal neurons (Hauss-Wegrzyniak et al., 1998a; Hauss-Wegrzyniak et al., 2000a; Hauss-Wegrzyniak et al., 2002). Although sustained IL-1β expression in the FIV-Cre-injected IL-1β^{XAT} mouse is similarly associated with glial activation, recruitment of immune cells and compromised blood-brain barrier, our current immunofluorescence data support our previous report that found no overt evidence of neuronal loss or neuropathology in the hippocampus of activated IL-1β^{XAT} mice (Shaftel et al., 2007b). Indeed, our quantification of TUNEL positive neurons is most likely an overestimate of neuronal loss since the majority of cells "counted" as neurons did not show co-localization for NeuN. Therefore, our results suggest that the sustained neuroinflammatory response *per se* may impact learning and memory processes without obvious contribution of neuronal loss.

The mechanism by which IL-1β compromises hippocampal function has yet to be deciphered. However, IL-1 has been shown to influence hippocampal neurogenesis (Gemma et al., 2007), glutamate receptor expression (Lai et al., 2006a), and long-term potentiation (LTP) (Bellinger

et al., 1993; Griffin et al., 2006). An initial event that may be integral in the observed hippocampal pathophysiology is chronic IL-1β-induced activation of microglia and upregulation of inflammatory molecules. In addition to serving as a primary source of IL-1β, reactive microglia produce cytokines and chemokines that may become harmful with prolonged elevation (Streit et al., 2004). In fact, treatment with minocycline, an inhibitor of microglial activation, spares cognitive deficits associated with aging and neuropathology in animal models (Griffin et al., 2006; Choi et al., 2007; Fan et al., 2007; Liu et al., 2007). Our immunohistochemical and molecular analyses presented here highlight the increased presence of reactive microglia and expression of numerous inflammation-related genes following FIV-Cre injection. Thus, it is likely that hIL-1β-initiated microglial activation contributed to the observed impairments in spatial learning and memory.

IL-1β initiates an inflammatory cascade that includes upregulation of cyclooxygenase activity and prostaglandin (PG) production in mouse brain (Moore et al., 2004). Using a rat model, Hein et al. (2007) report that a hippocampal injection of PGE_2 following fear conditioning induced the same degree of impaired context memory as IL-1β administration. Supporting the hypothesis that IL-1β-stimulated PGE_2 production impairs memory processes, several studies have shown attenuation of IL-1β-related behavioral disturbances upon treatment with an inhibitor to cyclooxygenase (COX), the requisite enzyme for PG production (Shaw et al., 2005; Hein et al., 2007). As elevated PGE_2 has been detected in the IL-1β^{XAT} mice following Cre-injection (Bliss et al., 2007), future studies are required to determine whether COX activity and PGE_2 are responsible for the memory deficits reported here.

It should be noted that basal IL-1 signaling appears to have a beneficial, if not constitutive, role in learning and memory. Studies using central infusion of IL-1 receptor antagonist (IL-1ra) (Depino et al., 2004), administration of IL-1β converting enzyme (ICE; caspase-1) inhibitor (Gemma et al., 2005) and transgenic mice with altered expressions of IL-1 receptor (IL-1rKO) (Avital et al., 2003), have all reported memory deficits in hippocampal-dependent tasks in rodents. To clarify the "cost/benefit" characteristics of IL-1β, Goshen and colleagues (2007) described a U-shaped effect of IL-1β on hippocampal-dependent processes by reporting memory deficits upon intra-hippocampal administration of IL-1ra (IL-1 blockade) and high dose IL-1β (10 ng), while observing facilitated memory in rats receiving a low dose of IL-1β (1 ng) (Goshen et al., 2007). The observation of a significant memory retention deficit in IL-1β^{XAT} mice 48 hours following completion of acquisition suggests that the degree of IL-1β induction and the associated glial activation occurring 14 days after viral induction falls on the detrimental part of the U-curve. However, it is possible that the degree of individual hIL-1β induction may have served to improve memory in some mice, contributing to the wide variation in FIV-Cre performance and the modest overall effect on spatial acquisition and retention.

Our within-animal comparison of the retention memory performance and hippocampal expression of inflammatory genes including IL-1β, supports a recent clinical study that found a negative correlation between IL-1β levels and cognitive function in aged subjects from the PROSPER study (Trompet et al., 2008). Interestingly, linear regression analyses restricted to mice with hIL-β overexpression indicated that, among the genes of interest, only IL-1α was a significant predictor of memory performance in FIV-Cre-injected mice, further extending the role of this cytokine in rodent cognition (Banks et al. 2001). The lack of correlation among expression of other hIL-β-induced genes with retention index may suggest a threshold effect of inflammation where the probability of memory dysfunction increases once a certain degree of neuroinflammation is achieved. Ongoing studies will address this hypothesis by behaviorally-testing IL-1β^{XAT} mice at extended time points after FIV-Cre injection where inflammatory indices are substantial yet declining (Shaftel et al., 2007a).

Epidemiological studies have suggested that women show greater deterioration of cognitive abilities in AD (Henderson and Buckwalter, 1994; Buckwalter et al., 1996). Recent data propose that the degree of neuroinflammatory response is dependent on sex and circulating estrogen with female rodents showing an estrous cyclic-dependent exaggerated response to brain injury (Vegeto et al., 2006; Cordeau et al., 2008; Hua et al., 2008). In our study, we did find a sex difference in GFAP expression in FIV-GFP mice with female mice demonstrating a significant elevation of GFAP mRNA abundance relative to males (data not shown). However, we did not detect a main effect of sex or interaction effect of sex $\times$ treatment for any behavioral or molecular index across all animals. This lack of effect may be due to time point examined, sub-optimal sample size, or varying estrous stage across female mice, a factor known to influence spatial memory performance (Frick and Berger-Sweeney, 2001). Future investigation with increased subject numbers and estrous stage detection will be required to determine if there are sex differences in spatial performance of IL-1β^{XAT} mice.

Our water maze apparatus had a search ratio (tank diameter: platform) smaller than comparable studies in rats and mice, a factor that has been associated with steeper learning curves and greater difficulty in assessing learning (Vorhees and Williams, 2006). Therefore, our protocol may have been less sensitive to the effect of hIL-1β overexpression on spatial acquisition. To supplement modification of the spatial water maze dimensions, inclusion of additional memory paradigms such as object novelty or contextual fear learning may be warranted to fully characterize the hippocampus-dependent cognition in the IL-1β^{XAT} mouse model.

In conclusion, we demonstrate that hippocampal IL-1β overexpression in the IL-1β^{XAT} mouse is associated with mnemonic deficits on a spatial task. Performance on acquisition and retention trials were negatively correlated with glial activation and mRNA expression of pro-inflammatory molecules, validating this transgenic mouse as a suitable animal model to investigate the role of chronic neuroinflammation in age- and pathology-related cognitive dysfunction. Although the time point used in this study (14 days) is not directly comparable to the age-associated neuroinflammation that can occur over years in humans, this data set is the first to describe mnemonic deficits in the IL-1β^{XAT} mouse, providing a foundation for evaluation of memory following more extended durations of hIL-1β induction. In addition, the IL-1β^{XAT} mouse may be valuable in investigating IL-1β-related sensitivity in the context of stressful behaviors (Buchanan et al., 2008; Chen et al., 2008), the influence of chronic neuroinflammation on neurodegeneration, and the impact of pharmacological intervention on chronic IL-1β-mediated behavior.

Acknowledgments

Abbreviations included in text

AD   Alzheimer's disease

ANOVA   analysis of variance

CCR2   chemokine (C-C motif) receptor 2

COX   cyclooxygenase

CXCR2   chemokine (C-X-C motif) receptor 2

FIV-Cre   feline immunodeficiency virus-Cre recombinase protein

FIV-GFP   feline immunodeficiency virus-green fluorescent protein

GFAP   glial fibrillary acidic protein

Iba-1   ionized calcium binding adaptor molecule-1

IL-1α   interleukin-1α

IL-1β   interleukin-1β

IL-1ra   interleukin-1 receptor antagonist

KC   keratinocyte chemoattractant

LPS   lipopolysaccharide

MCP-1   monocyte chemoattractant protein-1

MHC-II   major histocompatibility complex II

MIP-2   macrophage-inflammatory protein-2

MWM   Morris water maze

PG   prostaglandin

SEM   standard error of the mean

tOD   threshold optical density

References

Avital A, Goshen I, Kamsler A, Segal M, Iverfeldt K, Richter-Levin G, Yirmiya R. Impaired interleukin-1 signaling is associated with deficits in hippocampal memory processes and neural plasticity. Hippocampus 2003;13:826–834. [PubMed: 14620878]

Banks WA, Farr SA, La Scola ME, Morley JE. Intravenous human interleukin-1alpha impairs memory processing in mice: dependence on blood-brain barrier transport into posterior division of the septum. J Pharmacol Exp Ther 2001;299:536–41. [PubMed: 11602664]

Barrientos RM, Higgins EA, Sprunger DB, Watkins LR, Rudy JW, Maier SF. Memory for context is impaired by a post context exposure injection of interleukin-1 beta into dorsal hippocampus. Behav Brain Res 2002;134:291–298. [PubMed: 12191816]

Beach TG, Sue LI, Walker DG, Lue LF, Connor DJ, Caviness JN, Sabbagh MN, Adler CH. Marked microglial reaction in normal aging human substantia nigra: correlation with extraneuronal neuromelanin pigment deposits. Acta Neuropathol 2007;114:419–424. [PubMed: 17639428]

Bellinger FP, Madamba S, Siggins GR. Interleukin 1 beta inhibits synaptic strength and long-term potentiation in the rat CA1 hippocampus. Brain Res 1993;628:227–234. [PubMed: 8313151]

Bliss SP, Shaftel SS, Olschowka JA, Kyrkanides S, O'Banion MK. Chronic hippocampal IL-1β expression elevates PGE2 production in a cyclooxygenase-1 dependent manner. Soc Neurosci Abstr 2007;57:17.

Buchanan JB, Sparkman NL, Chen J, Johnson RW. Cognitive and neuroinflammatory consequences of mild repeated stress are exacerbated in aged mice. Psychoneuroendocrinology 2008;33:755–765. [PubMed: 18407425]

Buckwalter JG, Rizzo AA, McCleary R, Shankle R, Dick M, Henderson VW. Gender comparisons of cognitive performances among vascular dementia, Alzheimer disease, and older adults without dementia. Arch Neurol 1996;53:436–439. [PubMed: 8624219]

Cagnin A, Brooks DJ, Kennedy AM, Gunn RN, Myers R, Turkheimer FE, Jones T, Banati RB. In-vivo measurement of activated microglia in dementia. Lancet 2001;358:461–467. [PubMed: 11513911]

Chen J, Buchanan JB, Sparkman NL, Godbout JP, Freund GG, Johnson RW. Neuroinflammation and disruption in working memory in aged mice after acute stimulation of the peripheral innate immune system. Brain Behav Immun 2008;22:301–311. [PubMed: 17951027]

Choi Y, Kim HS, Shin KY, Kim EM, Kim M, Kim HS, Park CH, Jeong YH, Yoo J, Lee JP, Chang KA, Kim S, Suh YH. Minocycline attenuates neuronal cell death and improves cognitive impairment in Alzheimer's disease models. Neuropsychopharmacology 2007;32:2393–2404. [PubMed: 17406652]

Conde JR, Streit WJ. Microglia in the aging brain. J Neuropathol Exp Neurol 2006;65:199–203. [PubMed: 16651881]

Cordeau P Jr, Lalancette-Hebert M, Weng YC, Kriz J. Live imaging of neuroinflammation reveals sex and estrogen effects on astrocyte response to ischemic injury. Stroke 2008;39:935–942. [PubMed: 18258827]

Depino AM, Alonso M, Ferrari C, del Rey A, Anthony D, Besedovsky H, Medina JH, Pitossi F. Learning modulation by endogenous hippocampal IL-1: blockade of endogenous IL-1 facilitates memory formation. Hippocampus 2004;14:526–535. [PubMed: 15224987]

Fan R, Xu F, Previti ML, Davis J, Grande AM, Robinson JK, Van Nostrand WE. Minocycline reduces microglial activation and improves behavioral deficits in a transgenic model of cerebral microvascular amyloid. J Neurosci 2007;27:3057–3063. [PubMed: 17376966]

Frick KM, Berger-Sweeney J. Spatial reference memory and neocortical neurochemistry vary with the estrous cycle in C57BL/6 mice. Behav Neurosci 2001;115:229–237. [PubMed: 11256446]

Gavilan MP, Revilla E, Pintado C, Castano A, Vizuete ML, Moreno-Gonzalez I, Baglietto-Vargas D, Sanchez-Varo R, Vitorica J, Gutierrez A, Ruano D. Molecular and cellular characterization of the age-related neuroinflammatory processes occurring in normal rat hippocampus: potential relation with the loss of somatostatin GABAergic neurons. J Neurochem 2007;103:984–996. [PubMed: 17666053]

Gemma C, Fister M, Hudson C, Bickford PC. Improvement of memory for context by inhibition of caspase-1 in aged rats. Eur J Neurosci 2005;22:1751–1756. [PubMed: 16197515]

Gemma C, Bachstetter AD, Cole MJ, Fister M, Hudson C, Bickford PC. Blockade of caspase-1 increases neurogenesis in the aged hippocampus. Eur J Neurosci 2007;26:2795–2803. [PubMed: 18001276]

Goshen I, Kreisel T, Ounallah–Saad H, Renbaum P, Zalzstein Y, Ben-Hur T, Levy-Lahad E, Yirmiya R. A dual role for interleukin-1 in hippocampal-dependent memory processes. Psychoneuroendocrinology 2007;32:1106–1115. [PubMed: 17976923]

Griffin R, Nally R, Nolan Y, McCartney Y, Linden J, Lynch MA. The age-related attenuation in long-term potentiation is associated with microglial activation. J Neurochem 2006;99:1263–1272. [PubMed: 16981890]

Griffin WS, Sheng JG, Roberts GW, Mrak RE. Interleukin-1 expression in different plaque types in Alzheimer's disease: significance in plaque evolution. J Neuropathol Exp Neurol 1995;54:276–281. [PubMed: 7876895]

Griffin WS, Nicoll JA, Grimaldi LM, Sheng JG, Mrak RE. The pervasiveness of interleukin-1 in alzheimer pathogenesis: a role for specific polymorphisms in disease risk. Exp Gerontol 2000;35:481–487. [PubMed: 10959036]

Griffin WS, Sheng JG, Royston MC, Gentleman SM, McKenzie JE, Graham DI, Roberts GW, Mrak RE. Glial-neuronal interactions in Alzheimer's disease: the potential role of a 'cytokine cycle' in disease progression. Brain Pathol 1998;8:65–72. [PubMed: 9458167]

Hauss-Wegrzyniak B, Vannucchi MG, Wenk GL. Behavioral and ultrastructural changes induced by chronic neuroinflammation in young rats. Brain Res 2000a;859:157–166. [PubMed: 10720625]

Hauss-Wegrzyniak B, Vraniak PD, Wenk GL. LPS-induced neuroinflammatory effects do not recover with time. Neuroreport 2000b;11:1759–1763. [PubMed: 10852239]

Hauss-Wegrzyniak B, Dobrzanski P, Stoehr JD, Wenk GL. Chronic neuroinflammation in rats reproduces components of the neurobiology of Alzheimer's disease. Brain Res 1998a;780:294–303. [PubMed: 9507169]

Hauss-Wegrzyniak B, Lukovic L, Bigaud M, Stoeckel ME. Brain inflammatory response induced by intracerebroventricular infusion of lipopolysaccharide: an immunohistochemical study. Brain Res 1998b;794:211–224. [PubMed: 9622633]

Hauss-Wegrzyniak B, Lynch MA, Vraniak PD, Wenk GL. Chronic brain inflammation results in cell loss in the entorhinal cortex and impaired LTP in perforant path-granule cell synapses. Exp Neurol 2002;176:336–341. [PubMed: 12359175]

Hein AM, Stutzman DL, Bland ST, Barrientos RM, Watkins LR, Rudy JW, Maier SF. Prostaglandins are necessary and sufficient to induce contextual fear learning impairments after interleukin-1 beta injections into the dorsal hippocampus. Neuroscience 2007;150:754–763. [PubMed: 18035502]

Henderson VW, Buckwalter JG. Cognitive deficits of men and women with Alzheimer's disease. Neurology 1994;44:90–96. [PubMed: 8290098]

Hua X, Lei M, Ding J, Han Q, Hu G, Xiao M. Pathological and biochemical alterations of astrocytes in ovariectomized rats injected with D-galactose: a potential contribution to Alzheimer's disease processes. Exp Neurol 2008;210:709–718. [PubMed: 18289535]

Lai AY, Swayze RD, El-Husseini A, Song C. Interleukin-1 beta modulates AMPA receptor expression and phosphorylation in hippocampal neurons. J Neuroimmunol 2006a;175:97–106. [PubMed: 16626814]

Lai YC, Shaftel SS, Miller JN, Tallents RH, Chang Y, Pinkert CA, Olschowka JA, Dickerson IM, Puzas JE, O'Banion MK, Kyrkanides S. Intraarticular induction of interleukin-1beta expression in the adult mouse, with resultant temporomandibular joint pathologic changes, dysfunction, and pain. Arthritis Rheum 2006b;54:1184–1197. [PubMed: 16572453]

Liu Z, Fan Y, Won SJ, Neumann M, Hu D, Zhou L, Weinstein PR, Liu J. Chronic treatment with minocycline preserves adult new neurons and reduces functional impairment after focal cerebral ischemia. Stroke 2007;38:146–152. [PubMed: 17122429]

Moore AH, O'Banion MK. Neuroinflammation and anti-inflammatory therapy for Alzheimer's disease. Adv Drug Deliv Rev 2002;54:1627–1656. [PubMed: 12453679]

Moore AH, Olschowka JA, O'Banion MK. Intraparenchymal administration of interleukin-1beta induces cyclooxygenase-2-mediated expression of membrane- and cytosolic-associated prostaglandin E synthases in mouse brain. J Neuroimmunol 2004;148:32–40. [PubMed: 14975584]

Mrak RE, Sheng JG, Griffin WS. Glial cytokines in Alzheimer's disease: review and pathogenic implications. Hum Pathol 1995;26:816–823. [PubMed: 7635444]

Murray CA, Lynch MA. Evidence that increased hippocampal expression of the cytokine interleukin-1 beta is a common trigger for age- and stress-induced impairments in long-term potentiation. J Neurosci 1998;18:2974–2981. [PubMed: 9526014]

Nichols NR, Day JR, Laping NJ, Johnson SA, Finch CE. GFAP mRNA increases with age in rat and human brain. Neurobiol Aging 1993;14:421–429. [PubMed: 8247224]

Perry VH, Matyszak MK, Fearn S. Altered antigen expression of microglia in the aged rodent CNS. Glia 1993;7:60–67. [PubMed: 8423063]

Shaftel SS, Griffin WS, O'Banion MK. The role of interleukin-1 in neuroinflammation and Alzheimer disease: an evolving perspective. J Neuroinflammation 2008;5:7. [PubMed: 18302763]

Shaftel SS, Kyrkanides S, Olschowka JA, Miller JN, Johnson RE, O'Banion MK. Sustained hippocampal IL-1 beta overexpression mediates chronic neuroinflammation and ameliorates Alzheimer plaque pathology. J Clin Invest 2007a;117:1595–1604. [PubMed: 17549256]

Shaftel SS, Carlson TJ, Olschowka JA, Kyrkanides S, Matousek SB, O'Banion MK. Chronic interleukin-1beta expression in mouse brain leads to leukocyte infiltration and neutrophil-independent blood brain barrier permeability without overt neurodegeneration. J Neurosci 2007b; 27:9301–9309. [PubMed: 17728444]

Shaw KN, Commins S, O'Mara SM. Lipopolysaccharide causes deficits in spatial learning in the watermaze but not in BDNF expression in the rat dentate gyrus. Behav Brain Res 2001;124:47–54. [PubMed: 11423165]

Shaw KN, Commins S, O'Mara SM. Cyclooxygenase inhibition attenuates endotoxin-induced spatial learning deficits, but not an endotoxin-induced blockade of long-term potentiation. Brain Res 2005;1038:231–237. [PubMed: 15757639]

Sparkman NL, Martin LA, Calvert WS, Boehm GW. Effects of intraperitoneal lipopolysaccharide on Morris maze performance in year-old and 2-month-old female C57BL/6J mice. Behav Brain Res 2005a;159:145–151. [PubMed: 15795008]

Sparkman NL, Kohman RA, Scott VJ, Boehm GW. Bacterial endotoxin-induced behavioral alterations in two variations of the Morris water maze. Physiol Behav 2005b;86:244–251. [PubMed: 16115658]

Stalder AK, Carson MJ, Pagenstecher A, Asensio VC, Kincaid C, Benedict M, Powell HC, Masliah E, Campbell IL. Late-onset chronic inflammatory encephalopathy in immune-competent and severe combined immune-deficient (SCID) mice with astrocyte-targeted expression of tumor necrosis factor. Am J Pathol 1998;153:767–783. [PubMed: 9736027]

Streit WJ, Mrak RE, Griffin WS. Microglia and neuroinflammation: a pathological perspective. J Neuroinflammation 2004;1:14. [PubMed: 15285801]

Trompet S, de Craen AJ, Slagboom P, Shepherd J, Blauw GJ, Murphy MB, Bollen EL, Buckley BM, Ford I, Gaw A, Macfarlane PW, Packard CJ, Stott DJ, Jukema JW, Westendorp RG. Genetic variation in the interleukin-1 beta-converting enzyme associates with cognitive function. The PROSPER study. Brain 2008;131:1069–1077. [PubMed: 18304957]

Vegeto E, Belcredito S, Ghisletti S, Meda C, Etteri S, Maggi A. The endogenous estrogen status regulates microglia reactivity in animal models of neuroinflammation. Endocrinology 2006;147:2263–2272. [PubMed: 16469811]

Vorhees CV, Williams MT. Morris water maze: procedures for assessing spatial and related forms of learning and memory. Nat Protoc 2006;1:848–858. [PubMed: 17406317]

Weaver JD, Huang MH, Albert M, Harris T, Rowe JW, Seeman TE. Interleukin-6 and risk of cognitive decline: MacArthur studies of successful aging. Neurology 2002;59:371–378. [PubMed: 12177370]

Wingren AG, Bjorkdahl O, Labuda T, Bjork L, Andersson U, Gullberg U, Hedlund G, Sjogren HO, Kalland T, Widegren B, Dohlsten M. Fusion of a signal sequence to the interleukin-1 beta gene directs the protein from cytoplasmic accumulation to extracellular release. Cell Immunol 1996;169:226–237. [PubMed: 8620550]

Wu CW, Chen YC, Yu L, Chen HI, Jen CJ, Huang AM, Tsai HJ, Chang YT, Kuo YM. Treadmill exercise counteracts the suppressive effects of peripheral lipopolysaccharide on hippocampal neurogenesis and learning and memory. J Neurochem 2007;103:2471–2481. [PubMed: 17953674]

Yirmiya R, Winocur G, Goshen I. Brain interleukin-1 is involved in spatial memory and passive avoidance conditioning. Neurobiol Learn Mem 2002;78:379–389. [PubMed: 12431424]
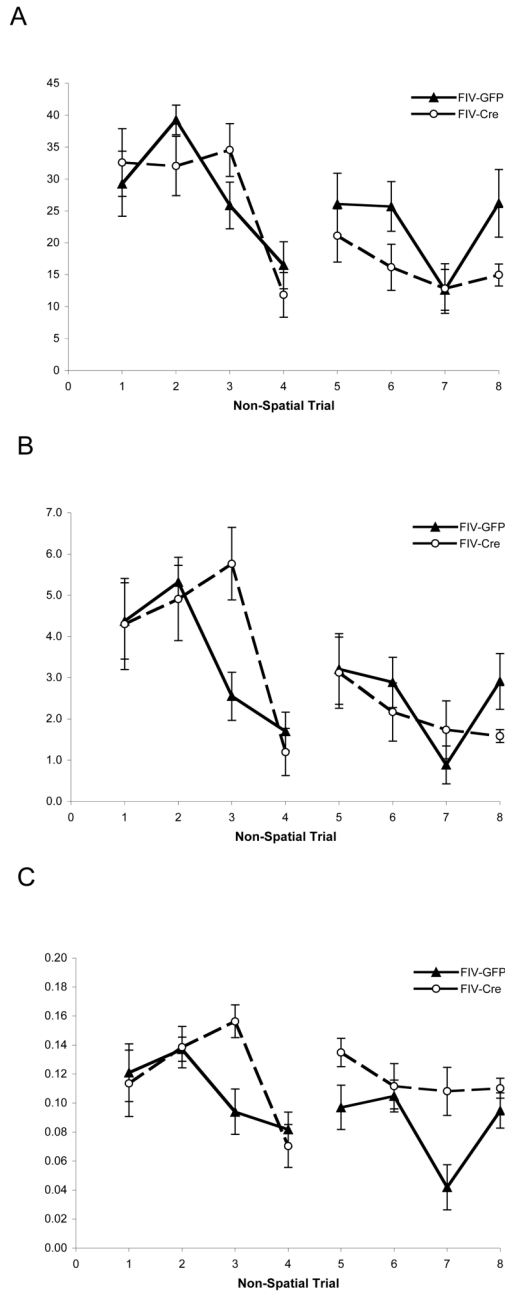
A

B

C

Figure 1.
Hippocampal hIL-1β transgene induction does not impact non-spatial task acquisition. Latency (A), path length (B), and swim speed (C) during the non-spatial water maze task. Each data point represents the mean ± standard error for each experimental group (n=9–12) for each trial, with better performance represented as lower latencies and path lengths. There was no significant effect of hippocampal IL-1β expression for any index.
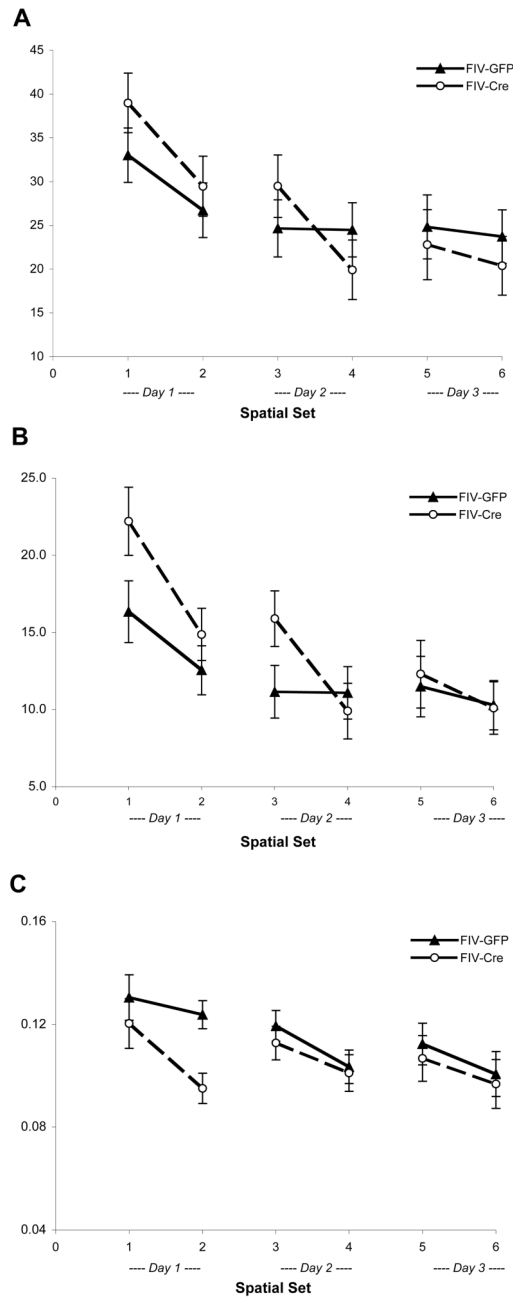
Figure 2.
Hippocampal IL-1β transgene induction impairs spatial acquisition. Latency (A), summed path length (B), and swim speed (C) during acquisition of the spatial water maze task. Each data point represents the mean ± standard error for each experimental group (n=9–12) during each set of 4 acquisition trials, with better performance represented as lower latencies and path lengths. A significant interaction between day × treatment was found for path length ($F_{2,19}=$ 4.05, p<0.05).
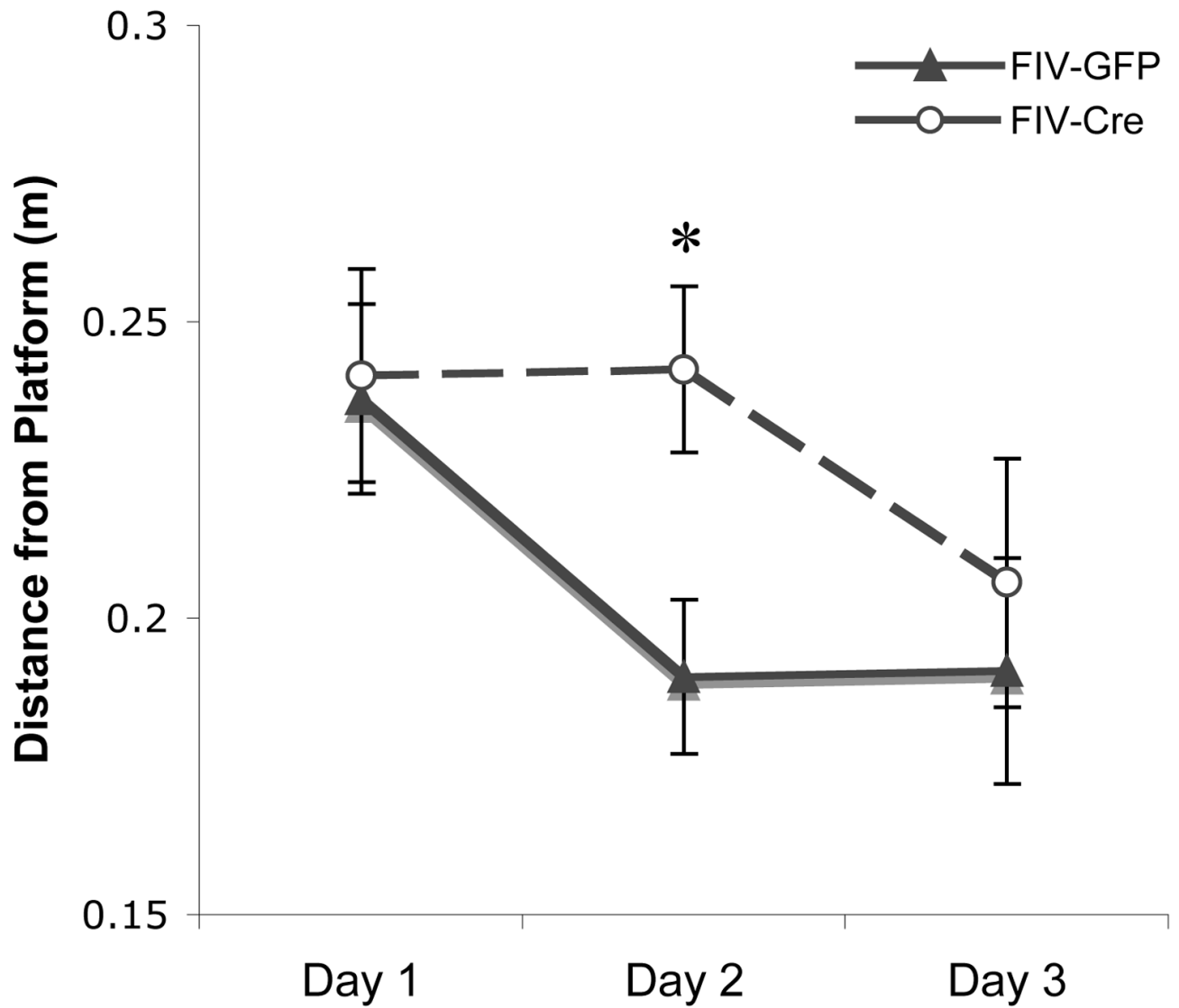
Figure 3.
FIV-Cre injected IL-1β^{XAT} mice spend greater distance from escape platform. Each data point represents mean distance from platform center per acquisition trial across all animals within each experimental group (± standard error). * indicates p<0.05.
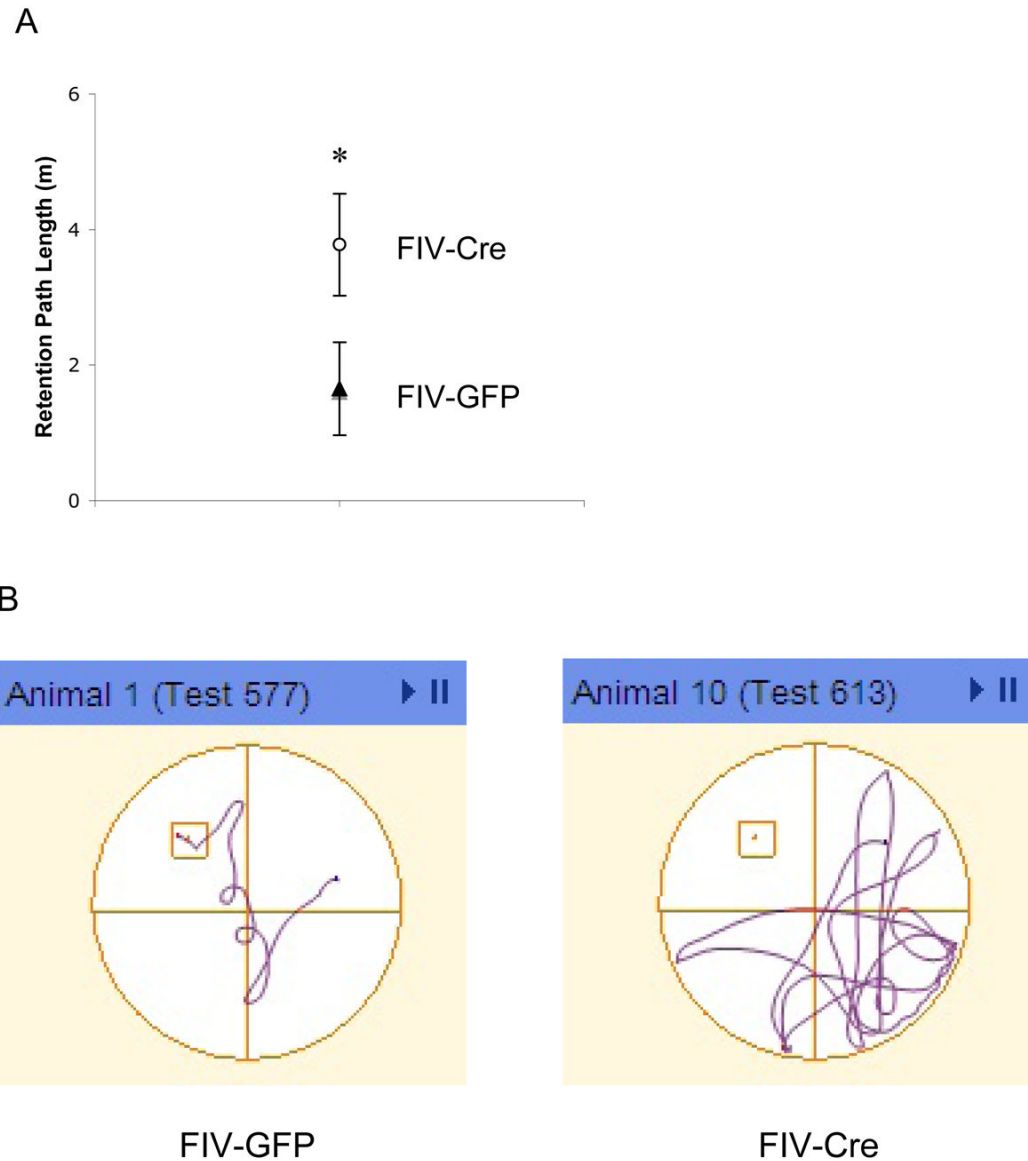
A

B

Figure 4.
Hippocampal hIL-1β transgene induction is associated with impaired spatial memory. (A) Forty-eight hours following acquisition training, FIV-Cre-injected IL-1β^{XAT} mice exhibited increased path lengths on the retention trial; * indicates p<0.05; n=9–12 per experimental group. (B) Test plots illustrating paths on retention trials. Each plot is from an individual mouse whose travel distance represents the mean of the denoted experimental group.
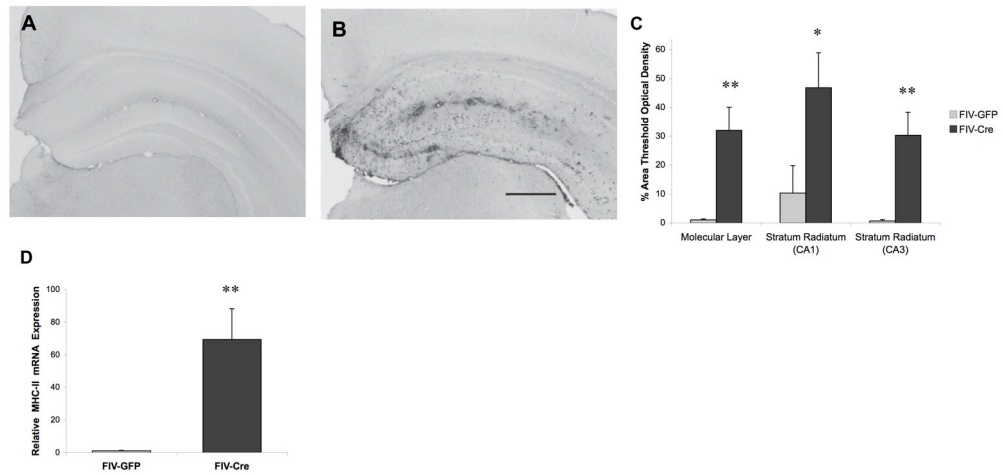
Figure 5.
Induction of hippocampal IL-1β leads to microglial activation. Microscopic observation of MHC class II immunoreactivity indicated increased staining intensity in hippocampus of FIV-Cre-injected mice (B) relative to FIV-GFP-injected (A) mice. Analysis evaluating percent of area reaching threshold optical density showed increased immunoreactivity in FIV-Cre hippocampal regions (C). Furthermore, real-time PCR showed elevated hippocampal MHC class II mRNA associated with FIV-Cre injection (D). ** indicates p<0.01, * indicates p<0.05 relative to FIV-GFP animals; n=9–12 per experimental group. Bar in B = 50 μm.
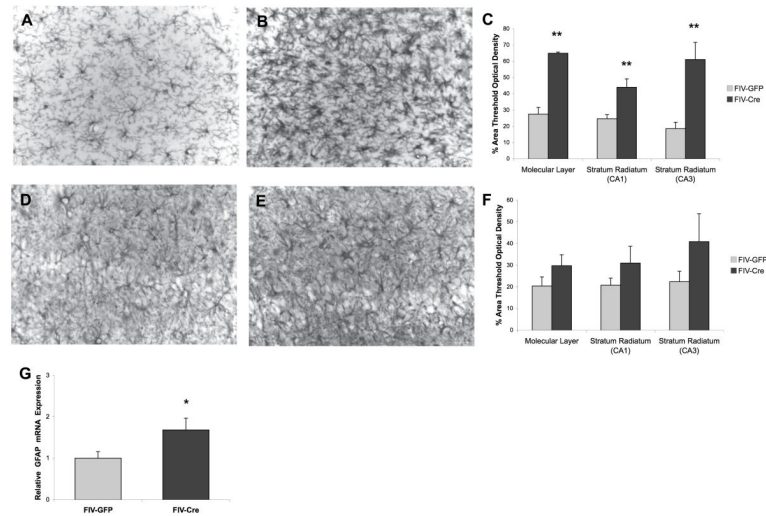
Figure 6.
Induction of hippocampal IL-1β leads to reactive gliosis. FIV-Cre-injected mice show evidence of microglial and astrocytic hypertrophy based on visual observation of Iba-1 and GFAP (B, E) immunoreactivity, respectively, relative to FIV-GFP-injected (A, D) mice. Analysis evaluating percent of area reaching threshold optical density showed increased immunoreactivity of Iba-1 (C) and GFAP (F) in FIV-Cre hippocampal regions. ** indicates $p < 0.01$ relative to FIV-GFP animals; n=4 per experimental group. Bar in E = 10 μm (G) Real-time PCR showed elevated hippocampal GFAP mRNA associated with FIV-Cre injection. * indicates $p < 0.05$ relative to FIV-GFP animals; n=9–12 per experimental group.
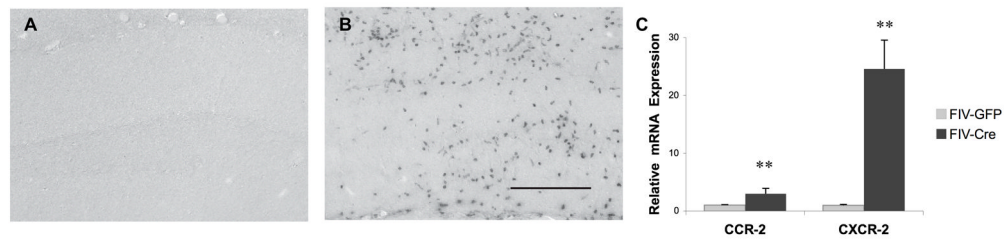
Figure 7.
Neutrophil infiltration is evident in FIV-Cre-injected mice. Positive staining of antibody 7/4 demonstrates presence of neutrophils associated with hIL-1β transgene induction (B) relative to FIV-GFP injected hippocampus (A). Bar in B = 20 μm. (C) Real-time PCR showed elevated hippocampal CCR-2 and CXCR-2 mRNA associated with FIV-Cre injection. ** indicates p<0.01 relative to FIV-GFP animals; n=9–12 per experimental group. Bar in E = 10 μm.
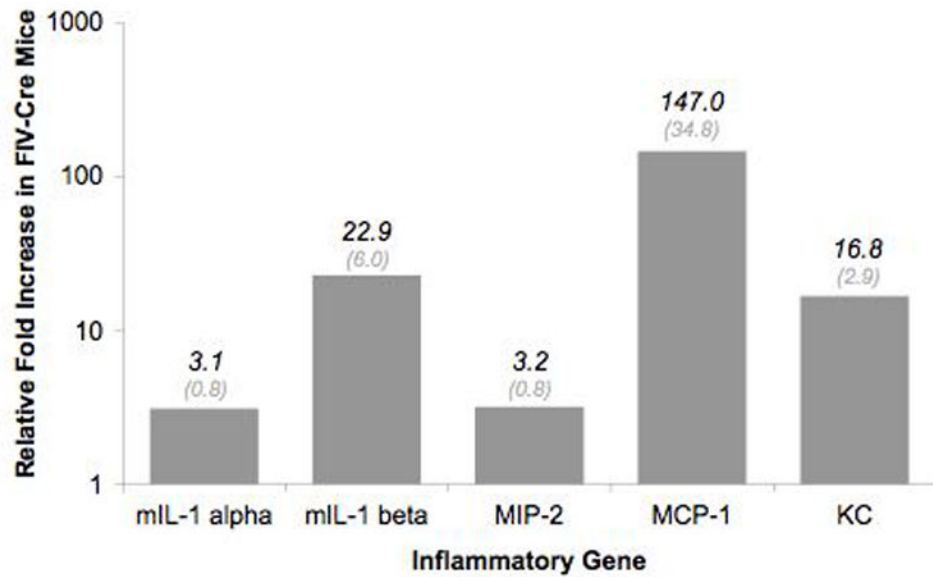
Figure 8.
Induction of hIL-1β mediates inflammation-related gene expression in the mouse hippocampus. qRT-PCR analysis revealed significant upregulation of all genes ($p < 0.05$; n= 9–12 per experimental group) in FIV-Cre-injected relative to FIV-GFP-injected IL-1β^{XAT} mice. One hippocampal sample from each mouse was analyzed. Expression of each gene was normalized to ribosomal 18s housekeeping gene. The graph represents normalized ratios of FIV-Cre mice relative to FIV-GFP-injected mice.
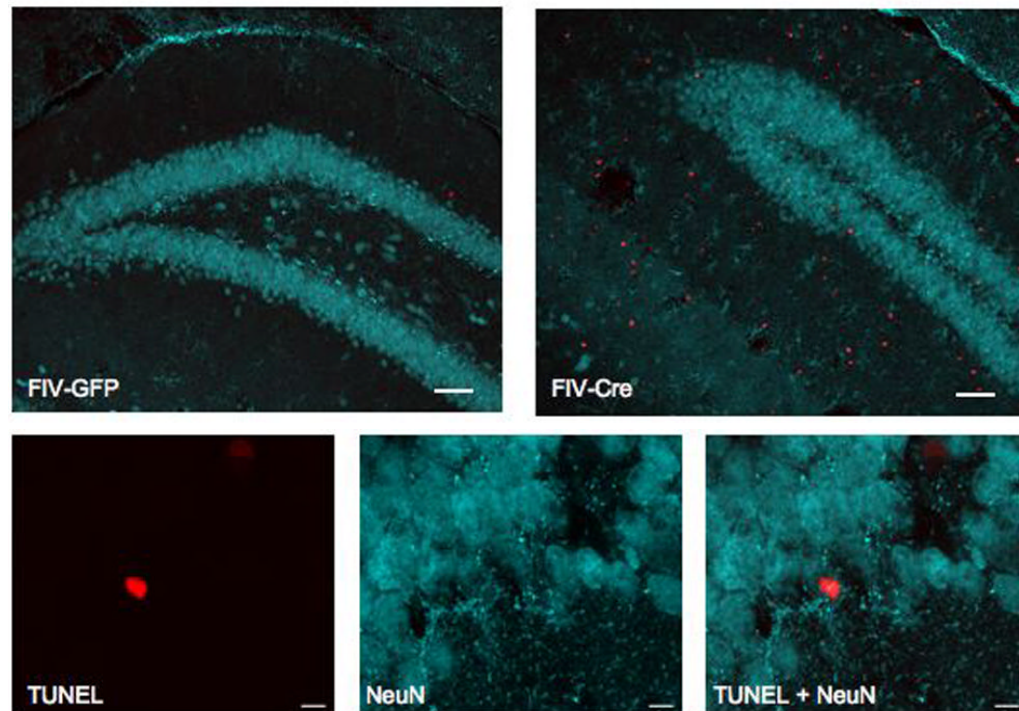
Figure 9.
Neuronal apoptosis is not associated with overexpression of hippocampal hIL-1β.
Representative images (20x) of dentate gyrus from FIV-GFP-injected (A) and FIV-Cre-injected mice stained with TUNEL (red) and NeuN (cyan), demonstrating increased number of TUNEL positive cells associated with hIL-1β induction. (C) High magnification (240x) of TUNEL immunoreactivity in FIV-Cre hippocampus demonstrates TUNEL positive cells in dentate gyrus granular cell layer.

Table 1

Primer sequences used for real-time quantitative PCR of mRNA expression in hippocampal tissue.

Gene		Primer sequences from 5′f to 3′f
GFAP	F	CTGGAGGTGGAGAGGGACAA
	R	GGTTGGTTTCATCTTGGAGCTT
	Probe	TTTGCACAGGACCTCGGCACCC
Murine IL-α	F	AAGGAGAGAGCCGGGTGACAGT
	R	GAAACTCAGCCGTCTCTTCTTCA
	Probe	CAGCAACGTCAAGCAACGGGAAGATTC
Murine IL-β	F	TCG CTC AGG GTC ACA AGA AA
	R	ATCAGAGGCAAGGAGGAAACAC
	Probe	CATGGCACATTCTGTTCAAAGAGAGCCTG
MIP-2	F	CAAGAACATCCAGAGCTTGAGTGT
	R	TTTTGACCGCCCTTGAGAGT
	Probe	CCCACTGCGCCCAGACAGAAGTCAT
MHC-II	F	AGTCAGTCGCAGACGGTGTTT
	R	GATAAGACAGCTTGTGGAAGGAATAGT
	Probe	TGAGACCAGCTTCTTCGTCAACCGTG
MCP-1	F	GGCTCAGCCAGATGCAGTTAA
	R	CCTACTCATTGGGATCATCTTGCT
	Probe	CCCCACTCACCTGCTGCTACTCATTCA
KC (CXCL1)	F	GCTAAAAGGTGTCCCCAAGTAA
	R	TAGGACCCTCAAAAGAAATTGTA
	Probe	CTGCTCTGATGGCACCGTCTGGT
CCR2		TaqMan® Gene Expression Assay (ID Mm99999051_gH; Applied Biosystems)
CXCR2	F	GTCTTTCAGCATGGCTCATTAC
	R	CGTGACCTCTTTCTCCCTGTA
	Probe	AGACTGTGGTATTTGAATTGATGCAGCC
18s rRNA	F	CGACCATAAACGATGCCGACT
	R	GTGGTGCCCTTCCGTCAA
	Probe	CGGCGGCGTTATTCCCATGACC